ELSEVIER

Thermochimica Acta 361 (2000) 113–120

thermochimica acta

www.elsevier.com/locate/tca

An introduction to μTA™ and its application to the study of interfaces

Rüdiger Häßler[a], Ekkehard zur Mühlen[b,*]

[a]*Institut für Polymerforschung Dresden e.V., Hohe Straße 6, D - 01069 Dresden, Germany*
[b]*TA Instruments GmbH, Max-Planck-Straße 11, D - 63755 Alzenau, Germany*

Received 2 February 2000; received in revised form 30 March 2000; accepted 31 March 2000

Abstract

Microthermal analysis (μTA™) combines the-high resolution visualization and positioning methods of scanning probe microscopy with the technology of thermal analysis. Equivalent to atomic force microscopy (AFM), the surface under investigation is scanned first to image its topography. Simultaneously, contrasts in thermal conductivity and/or thermal diffusivity across the surface of the sample are acquired. Based on these images specific locations are then selected for further thermal analysis (μTMA and μMDTA as local counterparts to thermomechanical, TMA, and modulated differential thermal analysis, MDTA).

In this article, the principles of μTA will be explained first; thereafter, the application of μTA to the studies of interfaces will be discussed. © 2000 Elsevier Science B.V. All rights reserved.

Keywords: Scanning probe thermal microscopy; Localized thermomechanical analysis; Localized differential thermal analysis; Interface; Interphase

---

1. Introduction

The methods of thermal analysis are well established with commonly recognized techniques for the characterization of morphological and compositional quantities of samples on a macroscopic scale. By acquisition of — as for example the enthalpy changes (in DSC or MDSC) — the weight of a sample (in TGA), the dimension or hardness of a sample (in TMA) as a function of temperature, information can be gained about the crystallinity, the amount of filler material or the cross-linking density of a sample. Samples with complex structures or samples exhibiting local variations in thermal properties throughout the dimensions of the sample lead to results in which measured values represent the average over the volume under investigation. The contributions of individual components or layers to a measured signal can be recognized, if they can be identified and separated by characteristic transition temperatures (e.g. temperatures of glass transitions, melting or decomposition) or the transition behavior (reversible vs. nonreversible heat flow in MDSC). With these methods, however, the spatial distribution of single phases, the thermal characterization of their interfaces and the study of the relation between morphological features and thermal properties is not possible in general. Thus, it is a rather promising approach to combine some

---

[*] Corresponding author. Tel.: +49-6023-9647-0; fax: +49-6023-9647-77.
E-mail address: ekkehard_zur_muehlen@tanst.waters.com (E.z. Mühlen).

PII: S0040-6031(00)00552-9

methods of thermal analysis with the unique capabilities of scanning probe microscopy.

2. Experimental

The most striking difference between µTA and a conventional AFM can be found in the different tip design: in µTA the AFM tip-cantilever assembly is replaced by a thin wire, from which cantilever and tip are formed (see Fig. 1). As the wire material, a so-called Wollaston wire is chosen, which consists of a 5-µm diameter Pt-core surrounded by a >50-µm thick Ag coating [1]. The immediate tip area is then freed from the coating, leaving only the small Pt-core exposed to form the tip. At the tip end this typically results in an area <1 µm×1 µm, which will be in contact with a surface during the investigation. The tip can now be heated by an electric current flowing through the wire. The generation of heat will be pronounced where the ohmic resistivity of the wire is large, which is the case at the very tip end. Here, the wire lacks the thick silver layer leaving only Pt with its small diameter. Furthermore, the resistivity will be increased at the position, where the Pt-core has been bent and pulled to form the V-shaped tip end. Finally, the temperature of the tip itself is a function of its ohmic resistivity, and thus it can be controlled by introducing the shown assembly into a Wheatstone bridge circuit.

In order to generate an image, the probing tip is brought into immediate contact with the surface thus operating in the region of repulsive forces. While the tip is stirred across the surface, changes in height within the topography will cause a deflection of the cantilever. This change in deflection is optically magnified by observing the motion of a laser beam, which is reflected off the upper side of the cantilever. This motion is finally monitored and converted into an electrical signal in a four-zone photodetector. During the imaging process, the feedback loop controls the vertical position of the cantilever mount to keep the deflection of the cantilever constant. Displaying this vertical position against the lateral position of the tip

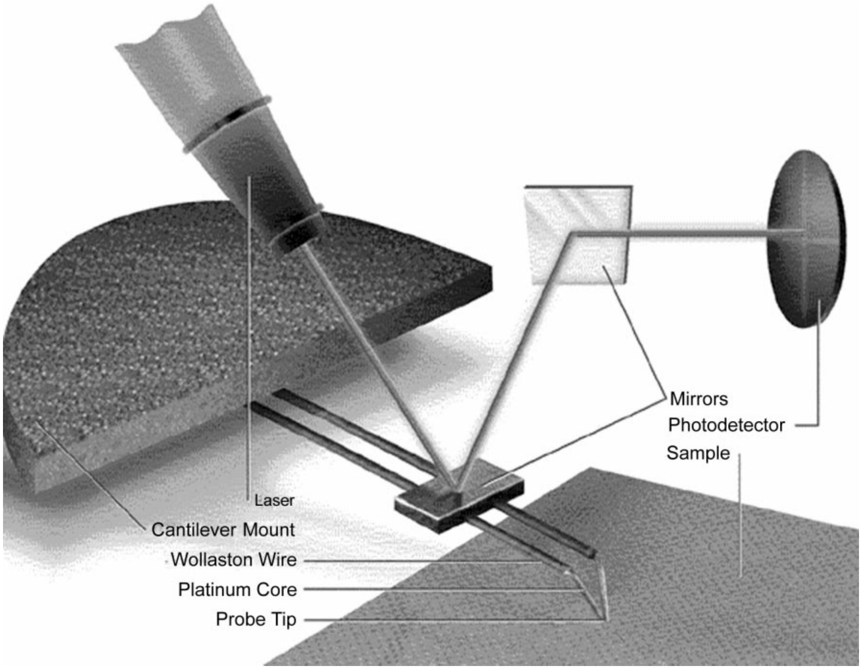

Fig. 1. Schematic design of µTA. In an AFM, the tip is replaced by a larger wire assembly which allows the acquisition of the temperature at the contact area to the surface. Simultaneously, it may act as a highly localized heater. The vertical deflection of the assembly is monitored by a light pointing technique.

within the scan-area results in an image of the topography, in which all three dimensions are quantified. The tip is stirred line-by-line across the surface to image a square scaning area.

The thermal properties of a sample surface can be simultaneously, acquired [1,2]: during the imaging process, the tip is in direct contact with the surface. Changes in thermal conductivity across the surface result in a different heat flow between tip and sample. Thus, changes in this property can be acquired by measuring the power level which is necessary to maintain the tip-temperature at a constant, preselected value. As this image is obtained isothermally the acquisition time is rather small. Typically, a scan is finished within a few minutes.

An illustration of the imaging capabilities can be found in Fig. 2. Shown are the topography and thermal conductivity images of the cross section of an ABS/PA (ABS — acrylonitrile/butadiene/styrene; PA — polyamide) interface. In the manufacturing process, PA is sprayed onto an ABS sheet at an elevated temperature. The temperature of PA is a critical parameter in the process, as it has to be high enough to melt the surface regions of the ABS sheet allowing the mixing of the two polymers in the interface. Indeed, the thermal conductivity image in Fig. 2 visualizes a gradual change of thermal conductivity across the interface of the two polymers. The conductivity is enhanced at the upper right of the image, as represented by bright gray values. It decreases slowly across the interface, and it may be derived from the image that the boundary between PA and ABS proceeds diagonally through the image, i.e. from the upper left to the lower right. It should be noted that this information cannot be obtained from the topography image in Fig. 2, which only shows the roughness of surface as it has been prepared by cutting.

For a further analysis locations can be selected within the images. The tip is then positioned at these locations, and it is then subject to a temperature program. Several signals can be acquired as a function of temperature:

μDTA curves display the power level necessary to keep the heating rate constant. The power is measured relative to a reference probe. As in macroscopic DTA or DSC measurements, an endothermal transition-like melting results in an increase of power consumption, as shown in the curves of Fig. 3. Displayed here is the melting of a PET (PET-polyethyleneterephtalate) surface. In this case, there is only a gradual change in power consumption throughout the temperature range, until melting of a surface phase occurs at a temperature of 528 K, consistent with the onset of the melting peak in macroscopic DSC measurements. Upon melting the power signal (here, shown as a derivative) rises sharply, followed by a decrease. The rise occurs when the tip penetrates into the melt. Once the force on the

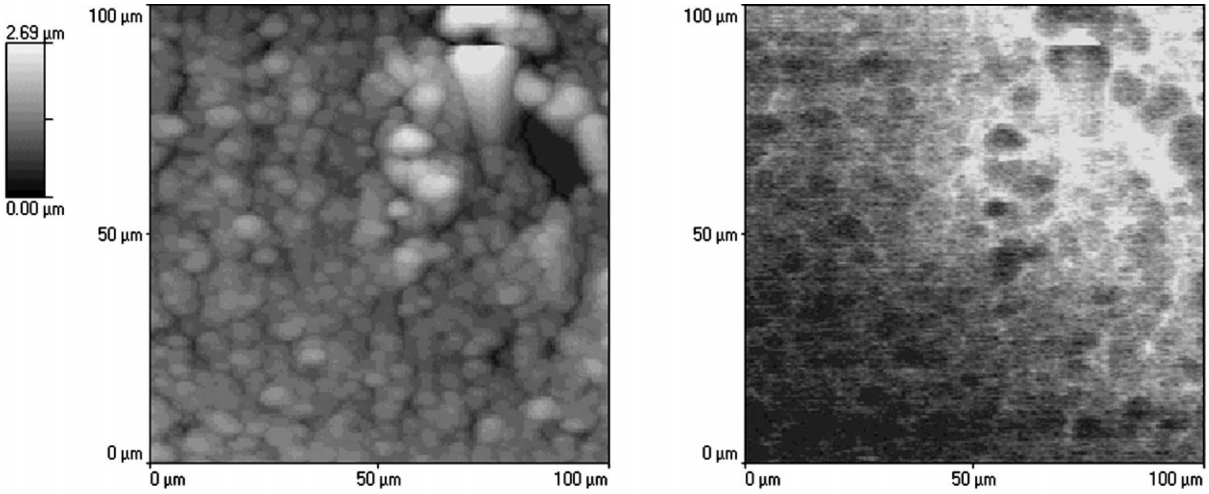

Fig. 2. Topography (left) and thermal conductivity (right) image of an interface between ABS and PA. The extension of the interface can be easily recognized in the conductivity image, while topography only reveals the quality of the surface after sample preparation.

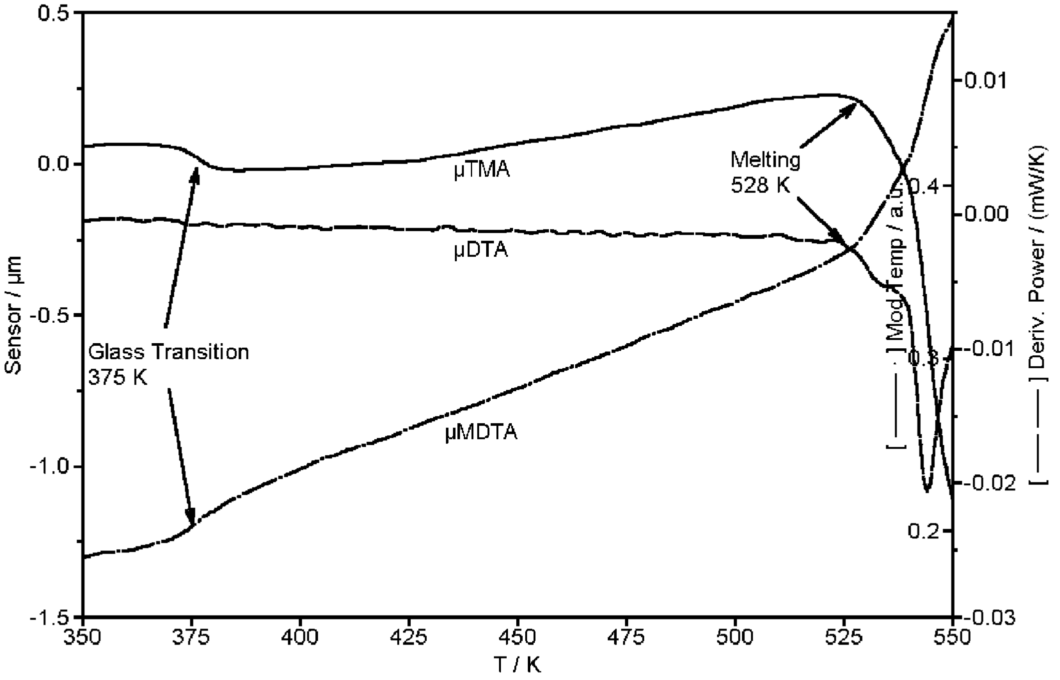

Fig. 3. µTMA, µDTA and µMDTA curves of a thin PET film. The µTMA and the µMDTA show the glass transition at 375 K, while all three signals clearly show the melting transition at 528 K.

cantilever is released, the tip looses contact to solid material causing the observed drop of the power value. Thus, the mechanism of peak formation is different from DSC. It should be emphasized that comparing the temperature onsets of transitions in this way leads to an agreement in results between DSC and µTA measurements.

The µMDTA curve shows the resistivity oscillation at the tip as caused by an AC power signal added to the temperature program [3]. The respective curve is also included in Fig. 3, showing a sharp transition during melting. This signal is especially useful during the study of those phase changes, which require only small amounts of power, but cause a larger change in heat capacity, as can be seen for the glass transition above 375 K.

Finally, µTMA curves display the change of the vertical displacement of the cantilever as a function of tip temperature. An expansion of the sample causes an increase in the value, and indeed the TMA signal rises before melting occurs in the curves displayed in Fig. 3. The value decreases if, for example the sample softens during melting with the result that the tip sinks into the sample. This signal is always obtained simultaneously with the µ(M)DTA signals, and the parallel interpretation makes it entirely possible to distinguish between different types of transitions.

Being finished with the investigation of a selected location, the tip is automatically raised from the surface, heated to a high temperature to decompose contamination, and positioned at the following selected area of interest. Last, but not the least, it should be mentioned that realised heating rates are rather high with typical values ranging between 2 and 10 K/s due to the low heat capacity involved at tip and sample. Typically sample areas with diameters ranging between 2 and 10 µm are affected during localised thermomechanical analysis (LTA), depending on the studied transition itself as well as on the acquisition parameters (force, final temperature, etc.).

3. Results and discussion

The capabilities of local thermal analysis experiments open up wide areas of applications, and a broad

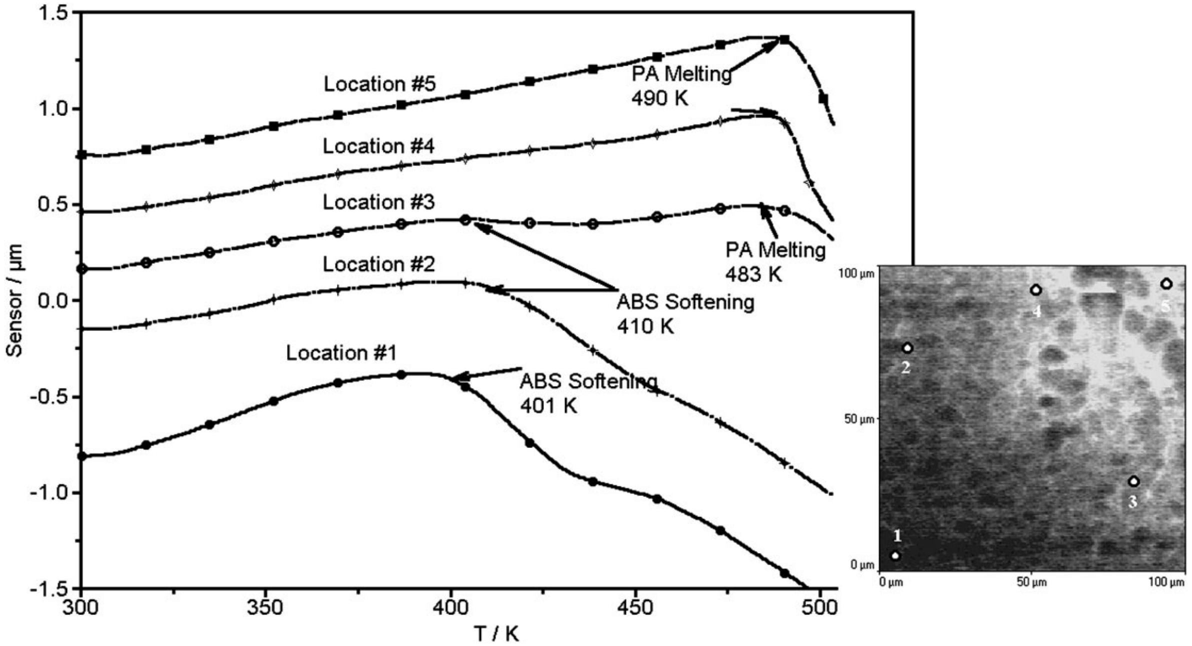

Fig. 4. µTMA curves of the interface shown in Fig. 2. The white circles show the selected locations for the LTA experiments as well as indicate the extension of analyzed material. Curves obtained at locations #1 and #2 show the behavior of ABS, while curves taken at locations #4 and #5 display the melting of PA at 490 K. In the interface, a curve with the softening of ABS as well as only a broad melting transition of PA can be observed.

range is already covered in the literature (e.g. [4–7]). In the following, this article will focus on studies of interface cross sections. At first, the study of the ABS/PA interface as introduced before will be discussed. Then, an example of T_g changes within a glue gap will be shown before the results obtained on a fiber/epoxy system are evaluated. In the latter two cases, the samples were cut and polished prior to investigation.

The µTMA curves measured at the ABS/PA interface, which has been introduced above, are summarized in Fig. 4. Next to the curves, the thermal conductivity image at the lower right shows the locations of the local thermal analysis experiments, as indicated by white circles. At a distance of about 50 µm from the interface, the µTMA curve resembles those measured at bulk ABS (Location #1). The material softens just above 400 K, as may be derived from the sudden change in slope of the corresponding µTMA curve. As the interface is approached, this temperature rises to values around 415 K (Location #2). As the mixing with polyamide occurs, this transition remains visible. However, a steep decrease of the slope does not come into effect until the polyamide component melts above 480 K (Location #3). This curve indicates that there is indeed a phase of mixed material present in the interface. Locations further away from the interface within the high conductivity area (locations #4 and #5) show melting transitions of polyamide starting at 490 K.

A thermal conductivity scan and the matching µTMA curves obtained from a faulty interface are summarized in Fig. 5. In contrast to the gradual change of conductivity shown in Figs. 2 and 4, the thermal conductivity scan shows a clear and well-defined boundary between the two components. On the low conductivity side, the softening temperature of ABS can be observed (e.g. 406 K at Location #1) everywhere, until an ≈10-µm wide layer close to the interface is analyzed (Location #2). There, the softening transition temperature has been reduced by >30 K, suggesting a de-mixing of the components of the ABS. On the high conductivity side, the observed melting temperatures are immediately higher than those measured at the aforementioned interface, thus indicating

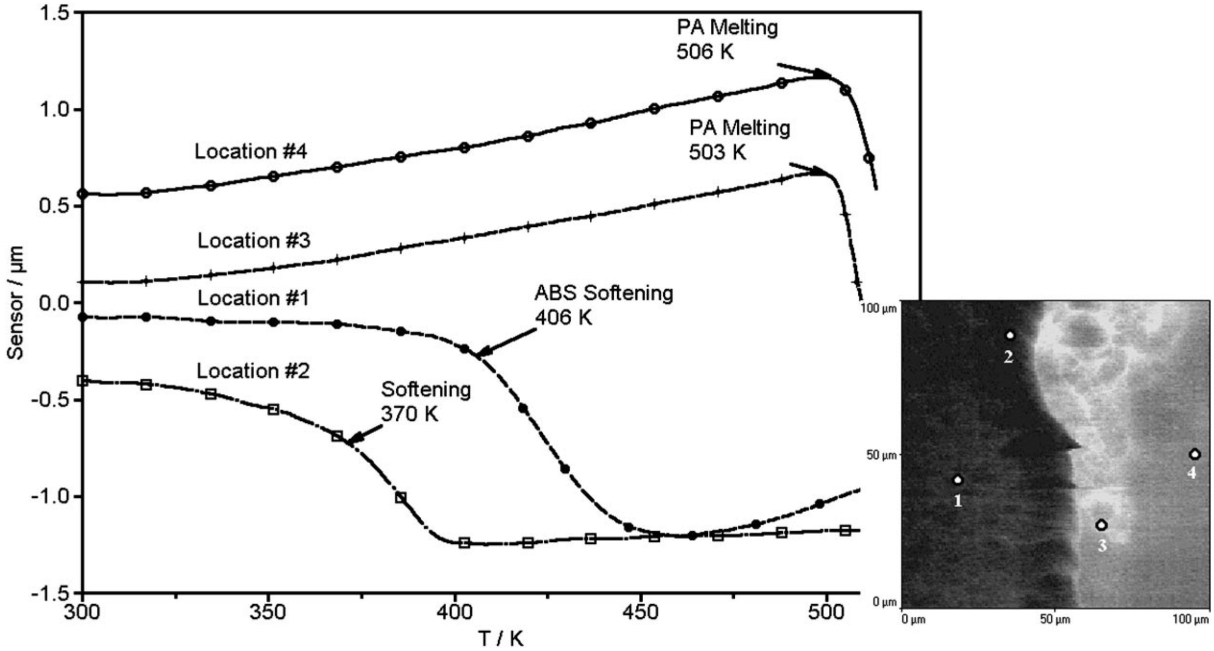

Fig. 5. µTMA curves taken at a faulty ABS/PA interface. The sample delaminates, and there is no mixing of the two materials in the interface. Thus, a sharp boundary can be observed and individual curves show either typical features of ABS or PA transitions.

a higher degree of crystallinity. The incomplete mixing of PA and ABS results in a delamination of both components, as they have largely different thermal expansion coefficients. It is most likely caused by a low processing temperature of polyamide, which allows only insufficient melting of the ABS surface.

Generally, the cross-linking density of a polymer is characterized by its glass transition temperature. With µTA, it is possible to measure these temperatures locally at selected positions on the sample surface. The glass transition causes a softening of the surface and, thus, the temperature can be well defined by monitoring changes in the µTMA signal during an LTA experiment. As the surface softens, the probing tip 'sinks' into the surface, resulting in a deviation of the signal from the expansion slope of the initially hard material.

Fig. 6 displays an example for such a measurement. The thermal conductivity image of the cross section of an epoxy/aluminum interface area is shown at the lower right. Prior to processing, the aluminum sheet was treated by an anodic oxidation in phosphorous acid [9]. This treatment results in an oxide layer at the surface of the sheet. Indeed, in the image a >5-µm wide area can be recognized (labeled '2') at the right next to the bulk metal (labeled '1'). The polymer is represented by dark gray values, indicating a drastically reduced thermal conductivity. Close to the interface between polymer and oxide layer (labeled '3'), the conductivity values of the polymer are increased compared with the bulk of the polymer (labeled '4').

A more quantitative analysis of the interface is possible using the local thermal analysis (LTA) capabilities of µTA. Results of µTMA measurements of the four indicated locations will be discussed, as summarized in the line diagram in Fig. 6. The curves obtained on bulk metal or at the oxide layer (locations #1 and #2) do only show thermal expansion without any transition. The slope of the µTMA signal measured at the oxide layer is significantly reduced due the lower thermal conductivity and the lower expansion coefficient of this layer. The µTMA curve obtained at the polymer in the immediate vicinity of the interface (Location #3) shows a significant softening transition around 411 K. Further in the bulk, the temperature of the softening transition decreases to values of 391 K (Location #4). This value agrees well with the results of T_g measured by DSC and DMA on pure epoxy samples.

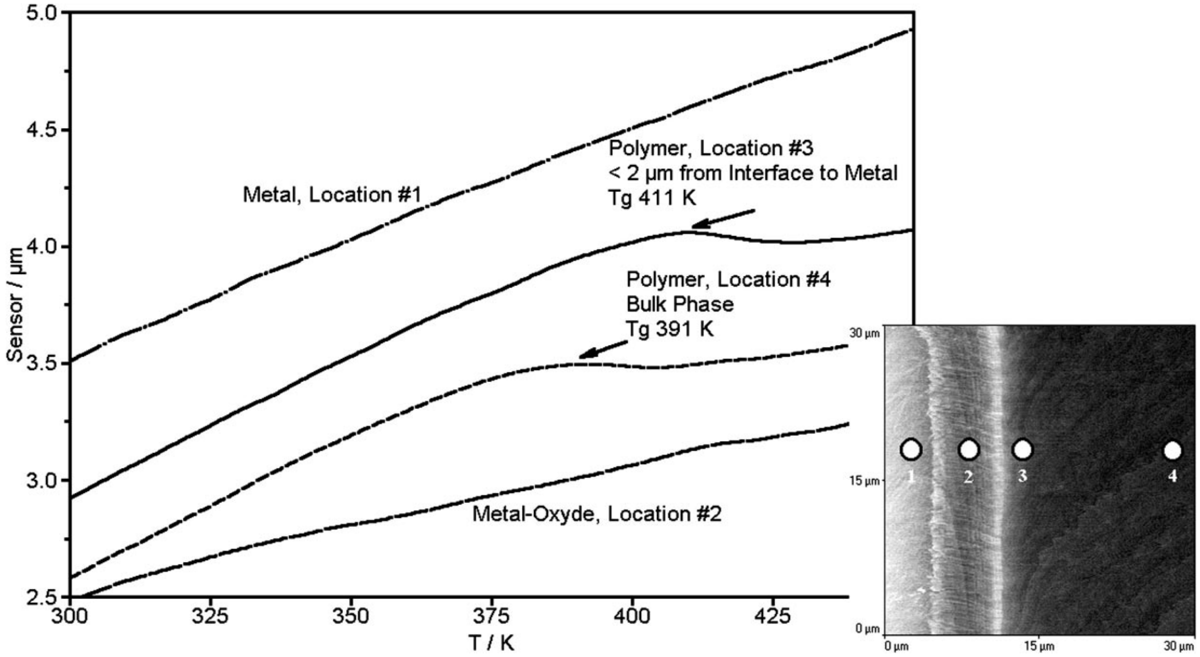

Fig. 6. µTMA curves taken at a metal–epoxy interface. Prior to treatment, the metal surface was oxidized, resulting in a 5-µm thick oxide layer. This layer can be easily recognized in the conductivity image, which covers a 30 µm wide scan area. The treatment of the surface influences the cross-linking behavior of the polymer and, indeed, the T_g of the polymer close to the interface is 20 K higher than the one measured in the bulk.

Thus, it may be concluded that the pre-treated surface has a significant impact on the cross-linking of the epoxy. The discussion remains whether the oxide layer plays an immediate role in the cross-linking of the polymer, as suggested in the literature.

The thermal conductivity image in Fig. 7 displays the contrasts between two embedded fibers, located in the center of the image, and the surrounding epoxy resin. Prior to embedding, the 13-µm diameter fibers were coated in a γ-APS/polyurethane sizing [8]. The embedding resin consists of an aminic hardening epoxy on a DGEBA base (Rütapox L20, Bakelite). The µTMA curve measured on the fiber shows only thermal expansion (Location #4). Just 1 µm from the fiber/epoxy interface, a softening transition at 428 K can be observed (Location #3). With increasing distance from the fiber, the temperature of the transition decreases to lower values, until the bulk value of 384 K can be measured (locations #2 and #1).

From the foregoing, it can be concluded that the cross-linking density of the epoxy surrounding the fiber is enhanced as compared to its bulk material. With µTA. it is entirely possible to quantify this enhancement by the observed rise in the temperature of the softening transition.

4. Conclusions and outlook

Combining the high-resolution positioning capabilities of scanning probe microscopy with some of the analytical techniques of thermal analysis opens up a wide range of novel applications. Images of topography and of contrasts in thermal conductivity allow the identification of different phases on a µm-scale. Subsequent local thermal analysis investigations reveal transition temperatures within the phases. Further areas of research will open up with the coupling to GCMS (GCMS-coupling of gas chromatography and mass spectrometry) [10] or IR (IR — infrared spectroscopy) [11], which have recently been demonstrated.

The technique has been applied successfully to the study of interfaces. It is possible to investigate and quantify the mixing of material on a molecular

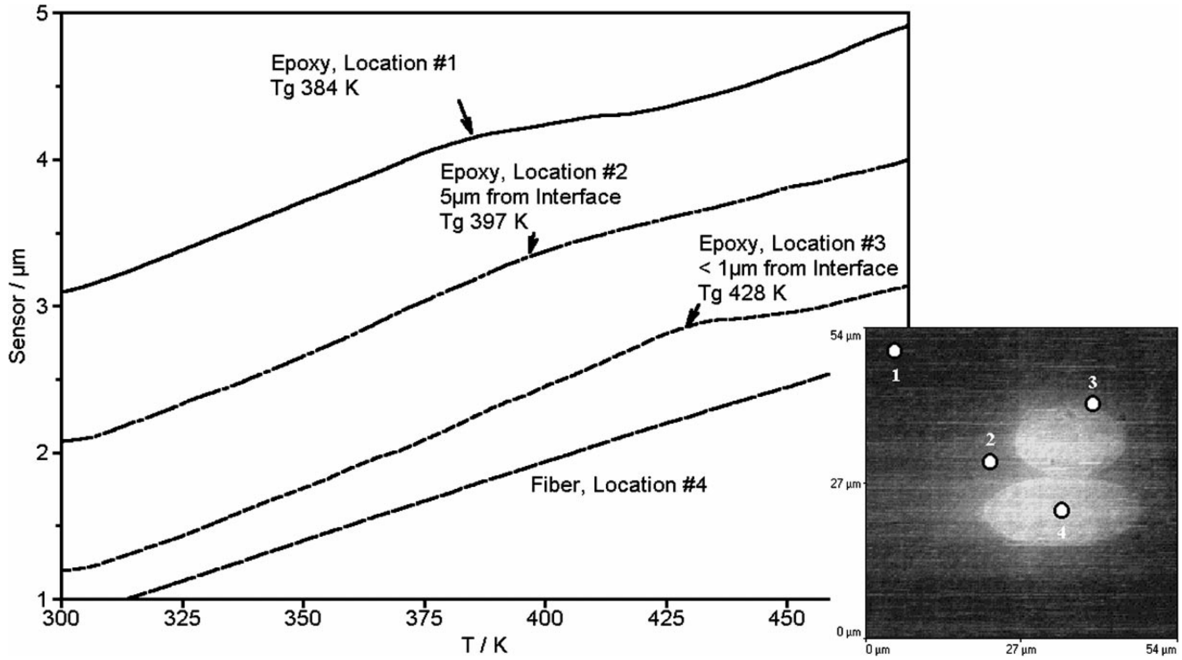

Fig. 7. Sized fibers embedded in an epoxy matrix. The fibers can be easily localized by their high values of thermal conductivity in the image. The epoxy itself softens at 384 K, as can be measured far from the interface between fiber and epoxy. As the interface is approached, the softening temperature rises to 428 K. This indicates a higher cross-linking density of the polymer in the immediate vicinity of the fiber.

level, which is crucial to an understanding of the delamination processes. Furthermore, studies of softening transition temperatures reveal information about the cross-linking behavior of polymer material close to interfaces. These studies are relevant to an understanding of the macroscopic mechanical properties of composite structures.

References

[1] R.B. Dinwiddie, R.J. Pylkki, P.E. West, Therm. Conductivity 22 (1994) 668.
[2] A. Hammiche, H.M. Pollock, D.J. Hourston, M. Reading, M. Song, J. Vac. Sci. Technol. B 14 (1996) 1486.
[3] A. Hammiche, M. Reading, H.M. Pollock, M. Song, D.J. Hourston, Rev. Sci. Instrum. 67 (1996) 4268.
[4] D.M. Price, M. Reading, A. Hammiche, H.M. Pollock, Thermochim. Acta. 332 (1999) 143.
[5] E. zur Mühlen, Rapra Book of Papers Developments in polymer analysis and characterisation (1999), Paper 2.
[6] E. zur Mühlen, Anwenderseminar Thermische Analyse, Ecomed (1999) 82.
[7] D.M. Price, M. Reading, A. Caswell, A. Hammiche, H.M. Pollock, M.G. Branch, Microsc. Anal. 65 (1998) 17.
[8] K. Mai, E. Mäder, M. Mühle, Composites Part A 29A (1998) 1111.
[9] R. Häßler, K. Mai, Kleben & dichten Adhäsion 42 (12) (1998) 24.
[10] D.M. Price, M. Reading, A. Hammiche, H.M. Pollock, Int. J. Pharm. 192 (1999) 85.
[11] A. Hammiche, H.M. Pollock, M. Reading, M. Claybourn, P. Turner, K. Jewkes, Appl. Spectrosc. 53 (1999) 810.